Int J Adv Manuf Technol (2018) 94:2667–2678
DOI 10.1007/s00170-017-1038-y

ORIGINAL ARTICLE

Design guideline for intermetallic compound mitigation in Al-Mg dissimilar welding through addition of interlayer

L. H. Shah[1,2] · **A. Gerlich**[1] · **Y. Zhou**[1]

Received: 9 June 2017 / Accepted: 29 August 2017 / Published online: 16 September 2017

Abstract This paper critically assesses the recent trends in aluminum-magnesium dissimilar welding and suggests a key design guideline to successfully improve the weld joint quality through addition of interlayer. First, the paper describes the main issue of incompatibility between these metals and considers the root cause of the problem, i.e., the Al-Mg-based intermetallic compounds (IMCs). It then reviews the recent trends of interlayer addition in various welding processes to mitigate Al-Mg IMCs. Focusing on laser welding, the paper finally proposes a 3-step design guideline in Al-Mg dissimilar welding through addition of an interlayer and presents a case study of using pure Ni foil as a proof of concept. The design guideline has shown to be an effective means to predict and prevent the formation of deleterious intermetallics.

Keywords Aluminum · Magnesium · Dissimilar welding · Intermetallic compound · Design guideline

1 Introduction

1.1 Dissimilar welding

Currently, a major portion of welding research has focused on dissimilar materials welding. The advantages of dissimilar materials welding are vast, such as weight reduction, cost reduction, energy efficiency, optimization of material use, and the ability to "tailor" the materials' design according to specific needs, commonly referred to as tailor-welded blanks in the automotive industry [1–4]. Welding processes for dissimilar metals will open up new industrial applications such as in the automotive, aerospace, energy, and medical sectors [5].

An increasing need in the automotive industry can be noted for dissimilar materials joining of aluminum and magnesium base metals. Individually, both metals have been widely used due to shared advantages such as light weight, high specific strength, high corrosion resistance, and recyclability. Dissimilar welding technology has provided the opportunity to exploit the advantages of both metals simultaneously in a multi-material component design [6].

However, similar to welding of aluminum and steel, Al-Mg welding is categorized as an incompatible dissimilar metal joining due to solubility issues, as will be explained in detail below [5]. Even so, the enormous potential for this combination has cast a spotlight on Al-Mg-joining research. As welding has always been an integral part of the automotive industry, the recent progress implies that a robust and reliable welding technique must be put forth to meet industrial demands.

This paper examines the fundamental issues which control the feasibility of dissimilar welding of Al to Mg alloys. Particularly, due to the growing availability of laser welding in the automotive industry, the paper focuses on laser welding and gives a critical review on the current research progress of using interlayers as an effective approach in improving joint quality. Through basic understanding of the material's thermodynamics, a 3-step general guideline to mitigate Al-Mg-based intermetallic compounds (IMCs) using interlayer material is proposed. Finally, a case study is conducted as a proof of concept of the interlayer guideline.

✉ L. H. Shah
lhahmads@uwaterloo.ca

[1] Centre for Advanced Materials Joining, Department of Mechanical and Mechatronics Engineering, University of Waterloo, 200 University Avenue West, Waterloo, ON N2L 3G1, Canada

[2] Faculty of Mechanical Engineering, Universiti Malaysia Pahang, Pekan, Pahang, Malaysia

1.2 Incompatibility between aluminum and magnesium

Figure 1 shows the equilibrium binary phase diagram of the Al-Mg system [7]. Although it is well known that the welding process in general is a non-equilibrium process [8], the equilibrium binary phase diagram is a useful tool to predict the reactions formed during welding and is regularly used as reference to determine if there is potential to achieve metallurgical bonding. The shaded areas in Fig. 1 show the only composition of aluminum and magnesium where a single-phase compound can be formed, i.e., successful solubility is achieved between aluminum and magnesium. From the trend of the graph lines, it can be predicted that at room temperature (not shown), the solubility of Al-Mg is negligible. Due to the extremely limited solubility between aluminum and magnesium, depending on the local composition, a mixture of aluminum or magnesium solid solution as well as Al_3Mg_2 and $Al_{12}Mg_{17}$ phases are likely to form during Al-Mg dissimilar welding, discussed in more detail as follows.

1.3 Intermetallic compound layer and its formation mechanism

It has been pointed out in most Al-Mg dissimilar laser welding papers that the greatest challenge to successful joining is the formation of Al_3Mg_2 and $Al_{12}Mg_{17}$ intermetallic compound layers at the interface of the base metals [6, 9–23]. These IMC layers will adversely affect the strength of the dissimilar joint due to its hard and brittle nature, with hardness values ranging from 152 to 221 HV [24]. This value is large compared to the nominal hardness values of pure aluminum and magnesium, between HV 25 and 60 [24].

To make matters worse, formation of the IMC at high temperatures is inevitable and impossible to prevent. Even with solid state welding where the general temperature is below the eutectic lines, diffusion reaction between Al and Mg atoms is expected, resulting in formation of both IMCs feasible in this binary system as continuous layers [25]. Yamamoto et al. [25] have demonstrated that, due to diffusion reaction, the overall IMC layer growth was so rapid that the layer becomes larger than 1 μm in a matter of seconds. Often, the IMC will form and thermal stresses lead to cracking upon cooling.

Since welding methods such as laser welding involves melting of the base metals in a non-equilibrium manner, it is obvious that such IMCs will form due to the excessive heat input generated by the heat source. It is therefore evident that only mitigation of such layers is possible.

1.4 Al-Mg dissimilar welding

The significance of Al-Mg dissimilar welding can be appreciated through the growing number of studies focusing on it using various welding methods. To date, successful joining of Al to Mg has been reported using metal inert gas (MIG) welding [26], laser welding [20, 21], friction stir welding (FSW) [27, 28], and resistance spot welding (RSW) [29, 30]. Several hybrid methods such as laser weld bond [12], laser + FSW [31], laser + TIG [10, 19, 22], and TIG + ultrasonic seam welding [32] have also been introduced to improve the welding outcome.

Hybrid approaches could prevent defects such as undercutting [10], while integrating effectively advantages of the two welding techniques due to different heat input and power densities [8, 33]. Improvements in the weld quality were reported from such hybrid techniques. However, hybrid welding requires a much more complex jig set up, increased complexity with additional processing parameters to consider, and comes with a cost trade-off. An alternative to the method above is using interlayer or filler metals between the base metals. This technique has gained popularity in recent years due to its cheap, simple but effective outcome to improve Al-Mg weld quality.

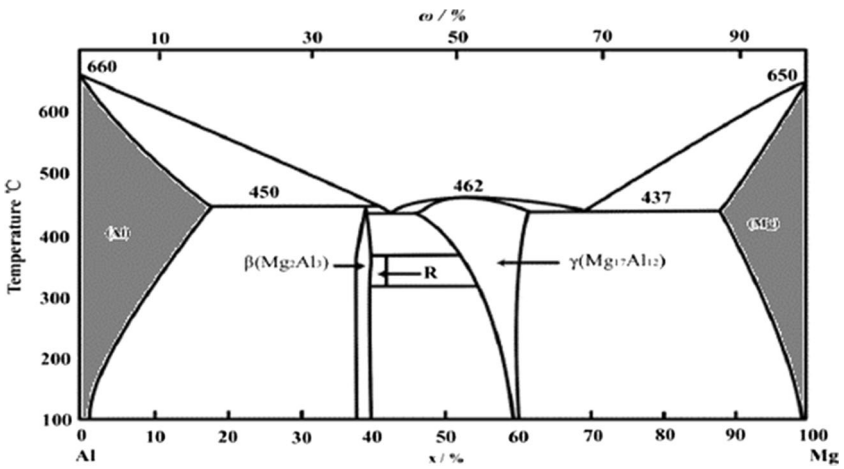

Fig. 1 Binary equilibrium phase diagram of the Al-Mg system [7]

2 Interlayer/filler addition as an effective solution

2.1 Al-Mg welding with interlayer

Table 1 outlines the recent trends towards utilizing interlayer or filler metal in Al-Mg dissimilar welding to attenuate the detrimental effects of Al-Mg-based IMCs. As can be seen, a variety of interlayer/filler metals were incorporated, including cerium, nickel, iron, tin, titanium, copper, zinc, and manganese. The concept behind this approach is simple; the metallic interlayer/filler is placed between the base metals during welding and acts as a substitute to replace Al-Mg reactions by developing reactions with aluminum, magnesium, or both base metals with the metallic interlayer during welding. This mechanism serves to limit the extent of Al-Mg reactions, consequently mitigating Al-Mg-based IMC phases.

This method has been proven effective in improving the dissimilar weld joint quality. For instance, Penner et al. (2014) used a unique approach by utilizing a Zn-coated steel interlayer between Al-Mg RSW. The higher melting point of the steel prevented it from melting and served as a barrier between the base metals while forming a metallic bond with the Zn coating [42]. Sun et al. (2016) also utilized a similar method on an AA5052-AZ31 dissimilar RSW by inserting a Sn-coated steel interlayer between the base metals. The mechanical property of the joint was reported to withstand load peaks as high as 88% of similar Mg RSW joints due to prevention of brittle Al-Mg IMCs [45]. These two examples demonstrate that suppression of Al-Mg-based IMCs can be attained through the interlayer's role as a "physical barrier" when its melting temperature is high enough to remain solid and avoid mixing between Al and Mg, or as "chemical barrier" where

Table 1 List of recent research progress on Al-Mg welding with interlayer/filler metal in chronological order

No.	Author	Year	Welding method	Configuration	Material (Al-Mg)	Interlayer/filler
1	L.M. Liu et al. [10]	2006	Laser + Tungsten inert gas (TIG)	Lap joint	AA6061 (bottom, b) and AZ31B (top, t)	Ce foil interlayer
2	W.S. Chang et al. [16]	2011	Nd:YAG laser + Friction stir welding (FSW)	Butt joint	A6061-T6 and AZ31B-H24	Pure Ni foil interlayer
3	X.D. Qi et al. [19]	2011	Nd:YAG laser + TIG	Lap joint	AA6061-T6 (b) and AZ31B (t)	St02Z mild steel foil interlayer
4	F. Scherm et al. [20]	2012	Nd:YAG laser	Lap joint	AA5754 (t) and AZ31 (b)	ZnAl filler metal
5	V.K. Patel et al. [34]	2012	Ultrasonic spot welding (USW)	Lap joint	AA5754 (t) and AZ31 (b)	Pure Sn interlayer
6	M. Gao et al. [21]	2012	Fiber laser	Lap joint	AA6061-T6 (b) and AZ31B (t)	Pure Ti interlayer + AZ31B filler wire
7	A. Panteli et al. [35]	2012	USW	Lap joint	AA6111-T4 (b) and AZ31-H24 (t)	Al coating
8	J. Shang et al. [36]	2012	Cold metal transfer welding (CMT)	Butt joint	AA6061 and AZ31B	Pure Cu filler metal
9	H. Wang et al. [22]	2013	Laser + TIG	Lap joint	AA6061 (b) and AZ31 (t)	Adhesive + Ni interlayer
10	H.Y. Wang et al. [23]	2013	Nd:YAG laser	Lap joint	AA6061 (b) and AZ31B (t)	Zn-coated Fe foil + adhesive
11	P. Penner et al. [37]	2013	Resistance spot welding (RSW)	Lap joint	AA5754 (t) and AZ31B (b)	Pure Ni/Au-coated Ni interlayer
12	F. Liu et al. [38]	2013	TIG	Butt joint	Al6061 and AZ31	Zn filler + pure Al foil
13	A. Panteli et al. [39]	2013	USW + cold spray	Lap joint	AA6111-T4 (b) and AZ31-H24 (t)	Al/Mn coating
14	H.T. Zhang et al. [26]	2014	Metal inert gas (MIG)	Butt joint	Al1060 and AZ31B	Zn-Cd alloy foil + Er4047 filler
15	H.T. Zhang et al. [40]	2014	Pre-rolled + TIG	Lap joint	AA6061 (t) and AZ31B (b)	Pure Zn interlayer
16	F. Liu et al. [41]	2014	TIG	Butt joint	6061 and AZ31	Zn29.5Al-0.5Ti filler metal
17	P. Penner et al. [42]	2014	RSW	Lap joint	AA5754 (top) and AZ31B (bottom)	Pure Zn/Zn-coated steel interlayer
18	Y. Zhang et al. [43]	2015	RSW	Lap joint	AA5052-H12 (top) and AZ31B (bottom)	Pure Zn interlayer
19	M. Sun et al. [44]	2015	RSW	Lap joint	AA5754-O (top) and AZ31B-H24 (bottom)	Pure Ni foil interlayer
20	M. Sun et al. [45]	2016	RSW	Lap joint	AA5052 (top) and AZ31B (bottom)	Sn-coated steel interlayer
21	X. Dai et al. [32]	2016	TIG + ultrasonic seam welding	Lap joint	Al6061 (top) and AZ31B (bottom)	Pure Zn interlayer

the presence of interlayers will preferentially favor the formation of alternative IMCs which are less detrimental. The chemical barrier aspect is discussed in detail in the next subsection.

Table 2 shows the summary of interlayer effects on the IMC formation and joint strength of Al-Mg laser welding. Despite the vast array of thin metallic interlayers utilized, all showed propitious improvements in joint strength, some even at par with the base metal. A coherent correlation can be seen between the enhancement of joint strength and the limited presence of brittle Al_3Mg_2 and $Al_{12}Mg_{17}$ IMCs, intentionally replaced by other less brittle intermetallics.

From Table 1, it is apparent that various metallic interlayers/fillers were suggested, with all cases showing enhancements in mechanical properties (partially shown in Table 2). Due to the shear simplicity of this method and the auspicious results, it therefore seems obvious that this approach is of great interest in future work.

However, a critical element that is missing in these cases is a proper guideline for choosing a certain interlayer. Most papers mentioned above give little mention to the reason a certain interlayer is chosen as oppose to others. Therefore, a thorough understanding of the governing principles behind the method may hold the key to designing a more systematic and robust approach in impeding Al-Mg-based IMCs, as will be discussed below.

2.2 The Miedema model

The improved results due to addition of metallic interlayers/fillers can be elegantly explained using the Miedema model. It was first proposed by Miedema (1979) to effectively calculate the standard molar enthalpy formation, ΔH, of all possible compounds [21, 46]. Three important parameters, namely the atomic size difference, the electron density mismatch, and the electronegativity difference are to be considered in the calculation, which is explained in detail elsewhere [46–50]. It is thus convenient to calculate and compare the formation enthalpies of all possible compounds formed during the welding process with the formation enthalpy values of the Al-Mg system.

2.3 Formation enthalpy of IMCs

The formation enthalpy of possible IMCs was calculated using a Miedema model-based software developed by Zhang et al. [48–52]. Figures 2 and 3 show the calculated formation enthalpies for different compositions of Al-Mg and Mg-Al, respectively, in comparison with other reported IMC formations in the literatures above (Table 1). Note that Fig. 3 shows less possible IMC formation, due to very limited interaction between Mg and the interlayer elements [19, 21, 22].

All other binary systems consistently and conclusively show a much lower formation enthalpy compared to the Al-Mg or Mg-Al baseline values, indicating that compounds other than Al-Mg prefer to form in a ternary system between Al, Mg, and the other constituent element. Thus, it is an effective means of suppressing formation of brittle ordered Al-Mg-based intermetallics, by substituting them with a more ductile phase.

2.4 Gibbs energy of compounds

Although the Miedema model clearly demonstrates that the interlayers/fillers of Ni, Ti, Fe, Ce, and Zn could effectively reduce Al-Mg-based IMCs by means of substitution, it could not pinpoint the dominant compound to form from a given binary system. For example, regarding the Al-Ti binary phase diagram, the system consists of three possible phases, namely $AlTi_3$, AlTi, and Al_3Ti. It is therefore equally critical to determine which would be the dominating phase to form, since each IMC exhibits distinct characteristics, and formation of

Table 2 Summary of interlayer effects on IMC formation and joint strength in Al-Mg laser welding [10, 16, 19–23]

Author	Year	Interlayer	Interlayer thickness	IMC formation	Maximum joint strength	Strength increase
L.M. Liu et al.	2006	Cerium foil	0.16–0.26 mm	Not specified	55.8 MPa (shear)	54.9%
W.S. Chang et al.	2011	Pure Ni foil	0.5 mm	NiAl and Ni_2Mg	169 MPa (tensile)	66%
X.D. Qi et al.	2011	St02Z mild steel foil	0.07–0.22 mm	$Mg_{17}Al_{12}$, Fe_2Al_5, and $FeAl_3$	100 MPa (shear)	284.6%
F. Scherm et al.	2012	ZnAl filler metal	1.6 mm (filler diameter)	Not specified	80 MPa (shear)	100% of Al base metal
M. Gao et al.	2012	Pure Ti foil + AZ31B filler wire	0.03–0.15 mm	Al_3Ti, $AlTi_3$, and $Al_{18}Ti_2Mg_3$	78.2 ± 3.6 MPa (shear)	60% of Mg base metal
H.Y. Wang et al.	2013	Zn-coated Fe foil (+ adhesive)	0.05 mm (Zn layer > 10 μm)	Not specified	101 MPa (shear)	75% of Mg base metal
H. Wang et al.	2013	Ni foil (+ adhesive)	0.08 mm	Mg_2Al_3, Mg_2Ni, and Al_3Ni	118 MPa (shear)	90.8% of Mg base metal

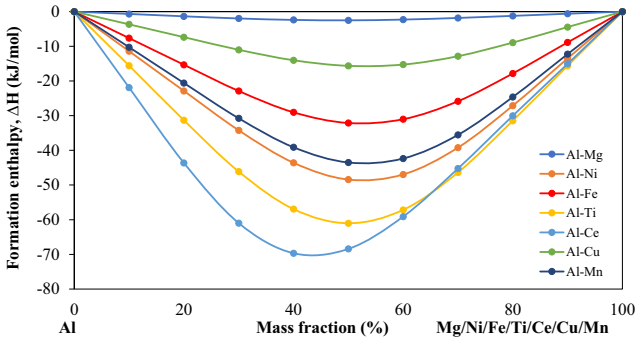

Fig. 2 Formation enthalpy, ΔH, of the Al-Mg, Al-Ni, Al-Fe, Al-Ti, Al-Ce, Al-Cu, and Al-Mn system as a function of mass fraction calculated by the Miedema model

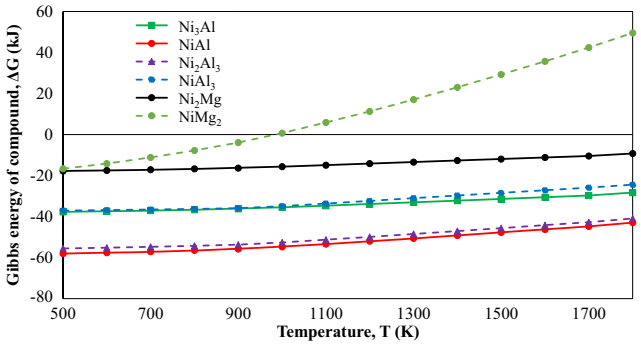

Fig. 4 Gibbs energy, ΔG, of different Al-Ni and Mg-Ni compounds as a function of temperature

brittle IMC similar or worse in nature compared to Al-Mg-based IMCs are obviously undesirable [53].

Gao (2012) and Wang (2013) have independently proved that the main phases to form in Al-Mg laser welding can be predicted by observing the Gibbs energy of compounds, ΔG, as a function of temperature diagram [21, 22, 54–56]. Based on such diagram, among all possible reactions, it is proposed that the reaction with the lowest ΔG will have the highest likelihood to take place. As an example, the Gibbs energy of Al-Ni- and Mg-Ni-based compounds for a binary Al-Ni/Mg-Ni system can be expressed using the diagram in Fig. 4 using HSC Chemistry 5.11 software [57].

From the above diagram, NiAl consistently shows the lowest Gibbs energy among all Al-Ni/Mg-Ni compounds regardless of temperature. Thus, when an Al-Mg-Ni ternary system is present, as in the case of Ni interlayer/filler addition [16, 22, 29, 44], NiAl will always be the dominant phase to form at any given temperature. However, this is not always the case, since Sun et al. (2015) reported observations of $NiAl_3$ on the Al/Ni interface, while Chang et al. (2011) suggested possible formation of Ni_2Mg and NiAl at the interface [16, 44]. Wang et al. (2013) also suggested the presence of $NiMg_2$ and Al_3Ni through EDS analysis of their work [23].

These contradicting observations can be explained through local compositions and the kinetics of the welding process. Although the Gibbs energy of compound serves well as a general reference, formation of IMCs relies heavily in the local composition during elemental interactions. For instance, a slight local depletion of Ni composition in an Al-Ni interaction may change a possible NiAl formation into a Ni_2Al_3 compound instead, particularly since both ΔGs are almost similar. Another reason for this inconsistency is due to the erratic and non-equilibrium nature of welding processes. The precise control of the welding kinetics is vital and challenging, since two incompatible base metals are involved.

The core concept of introducing interlayer is to not only inhibit interaction of Al to Mg but also substitute it with a less brittle intermetallic interface to allow limited amount of deformation before fracture. Since a compound's brittleness is often associated with its hardness value, a compound with lower hardness, i.e., more ductile compared to the Al-Mg IMCs, is therefore desirable. Considering the Al-Ni and Mg-Ni binary phase diagrams, the possible compounds to form and the respective hardness values are shown in Table 3. With the hardness of 152–221 HV as the baseline, the only compound to be of less hardness value is NiAl. Therefore, the formation of this

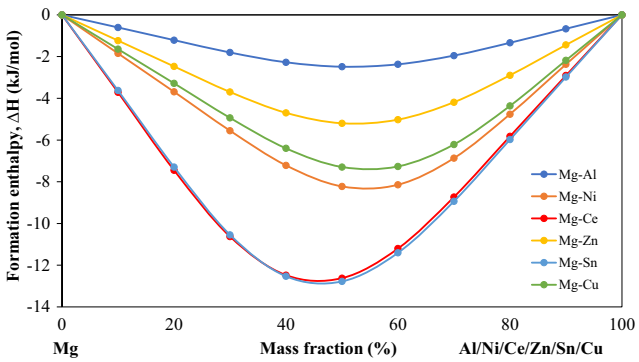

Fig. 3 Formation enthalpy, ΔH, of the Mg-Al, Mg-Ni, Mg-Ce, Mg-Zn, Mg-Sn, and Mg-Cu system as a function of mass fraction calculated by the Miedema model

Table 3 Possible compound formation between Al-Mg-Ni and its hardness values

Possible compounds	Hardness value (HV)	Reference
Al_3Mg_2 and $Al_{12}Mg_{17}$ (baseline)	152 to 221	[24]
NiAl	115.45	[58]
$NiAl_3$	441	[59]
Ni_2Al_3	759 ± 25	[60]
Ni_3Al	450.6	[61]
$NiMg_2$	459 ± 10	[62]
Ni_2Mg	646 ± 17	[62]

compound is preferred when Ni interlayers are utilized. Through theoretical explanations of formation enthalpy, Gibbs energy of formation and the less brittle nature of NiAl compounds, there is good theoretical grounds that this could be achieved. The final process is therefore to prove it through empirical data.

2.5 The 3-step Al-Mg-based IMC mitigation general design guideline

With the basic understanding of the governing principles mentioned above, a 3-step general guideline is proposed as shown in Fig. 5. Future endeavors in this field should consider these points if a better Al-Mg joint is desired.

Initially, a random interlayer is selected. In step 1, the thermodynamic aspect of the interlayer is assessed. The element's enthalpy of formation, ΔH, and Gibbs energy of compound, ΔG, are compared to the Al-Mg system. If both show lower values compared to the Al-Mg system, then the interlayer can be assessed through the next step. If this is not the case, the interlayer is deemed not suitable for the process and an alternative interlayer would be chosen.

Step 2 is the mechanical property and processing aspect. In this step, the relative brittleness of the expected compound to form is compared to the Al-Mg IMC hardness values. If the value has lower hardness, it is a good candidate to be considered. Passing these criteria provides good basis to perform initial feasibility studies on the effectiveness of an interlayer to attenuate the detrimental effect of Al-Mg IMCs. In addition, considering the high-power density of some fusion welding process, a high melting point interlayer could potentially act as a "physical barrier" and limit interaction between both metals. Since this method is expected to be practical, some other points that should also be taken into consideration is cost and accessibility.

The third and last step is the trial stage. This is equally critical in the design guideline because all welding processes are highly non-equilibrium and the outcome also heavily relies on the welding parameters. A suitable interlayer coupled with optimum parameters is expected to produce the best joint quality.

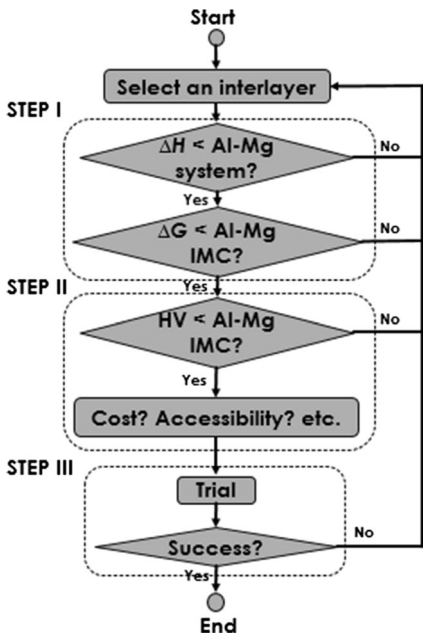

Fig. 5 The 3-step design guideline for interlayer selection in Al-Mg dissimilar welding

3 Proof of concept: Al-Mg laser welding with Ni interlayer

3.1 Experimental method

Through the assessments shown in Fig. 5, pure Ni foil has been selected as a good interlayer for this process. In addition, Ni interlayer was chosen based on accessibility, low cost, and having a high melting temperature (1455 °C) which doubles as a pseudo-physical barrier to limit rigorous mixing of base metals due to the intense heat input of the laser beam. Previous researches have also shown joint improvements in past dissimilar welding studies using resistance spot welding [29, 44, 63], hybrid laser-friction stir welding [16], hybrid laser-TIG welding [64], and laser-arc-adhesive hybrid welding [22].

Joining of aluminum alloy AA6022 (0.6 wt%Mg and 1 wt%Si) to magnesium alloy AZ31B (3 wt%Al and 1 wt%Zn) was successfully conducted with the addition of pure Ni based as the interlayer. The thickness of the base metals and Ni foil is 2 and 0.1 mm, respectively. Attempts to weld Al to Mg without Ni foil using several parameters were unsuccessful due to premature cracking during cooling. Laser welding is chosen due to several reasons; namely, laser beams offer a higher power density, indicating efficient welding process, high cooling rates, and shorter times for diffusion to limited IMC formation; and a sizable amount of successful case studies can be extracted from literature [10, 16, 19–23].

The process setup uses magnesium-on-top configuration. The laser welding was done in IPG Photonics, MI, USA, using a YLS-6000 fiber laser. The keyhole mode was utilized with argon as the shielding gas. The parameters of the laser welding are shown in Table 4.

Table 4 Process parameters of Al-Mg laser welding with Ni foil interlayer

Parameter	Value
Power (W)	1225
Weld speed (mm/s)	35
Focal length (mm)	200
Shielding gas	Argon

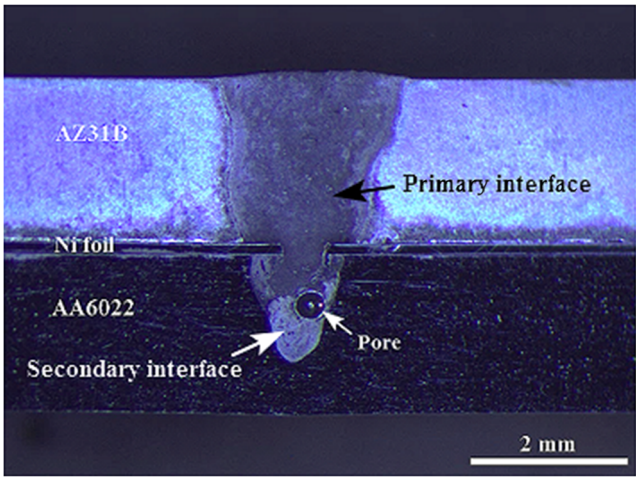

Fig. 6 Cross sectional macrograph of the laser welded sample

The sample was cut to observe the cross section of the weld region through optical microscope. It subsequently underwent X-ray energy dispersive spectroscopy (EDS) and X-ray diffraction (XRD) analysis for IMC composition and compound identification. For hardness measurements, a Vickers hardness test was conducted using 200 gf with 15 s dwell time.

3.2 Microstructural characterization

The cross-section macrograph of the welded sample is shown in Fig. 6. As can be seen in the cross section, a sound weld joint was produced with the weld region penetrating well into the bottom Al-alloy base metal. Two distinct interfaces can be observed, one dominating the entire Mg base metal and penetrating to the Al side (primary interface) and another interface dominating the Al base metal (secondary interface). No IMC layer was observed at the boundary layer between fusion zone and base metals. It could also be seen that the pure Ni foil also acted as a pseudo-barrier to limit interaction between the base metals as a "waist" was formed between the base metals. An observable defect is a single pore measuring approximately 4 μm in diameter caused by gas entrapment. Porosity is a common laser welding defect that is difficult to avoid [65–67].

The weld region of the sample was observed using EDS and an elemental mapping was conducted. Figure 7a shows the SEM image of the analysis region, while Fig. 7b–d shows the elemental mapping for Mg, Al, and Ni, respectively. In Fig. 7a, several Ni islands (bright areas) can be seen scattered throughout the interfacial region. In addition, a crack can also be observed forming beneath the left side of the Ni foil layer in the secondary interface, indicating the brittle nature of the region.

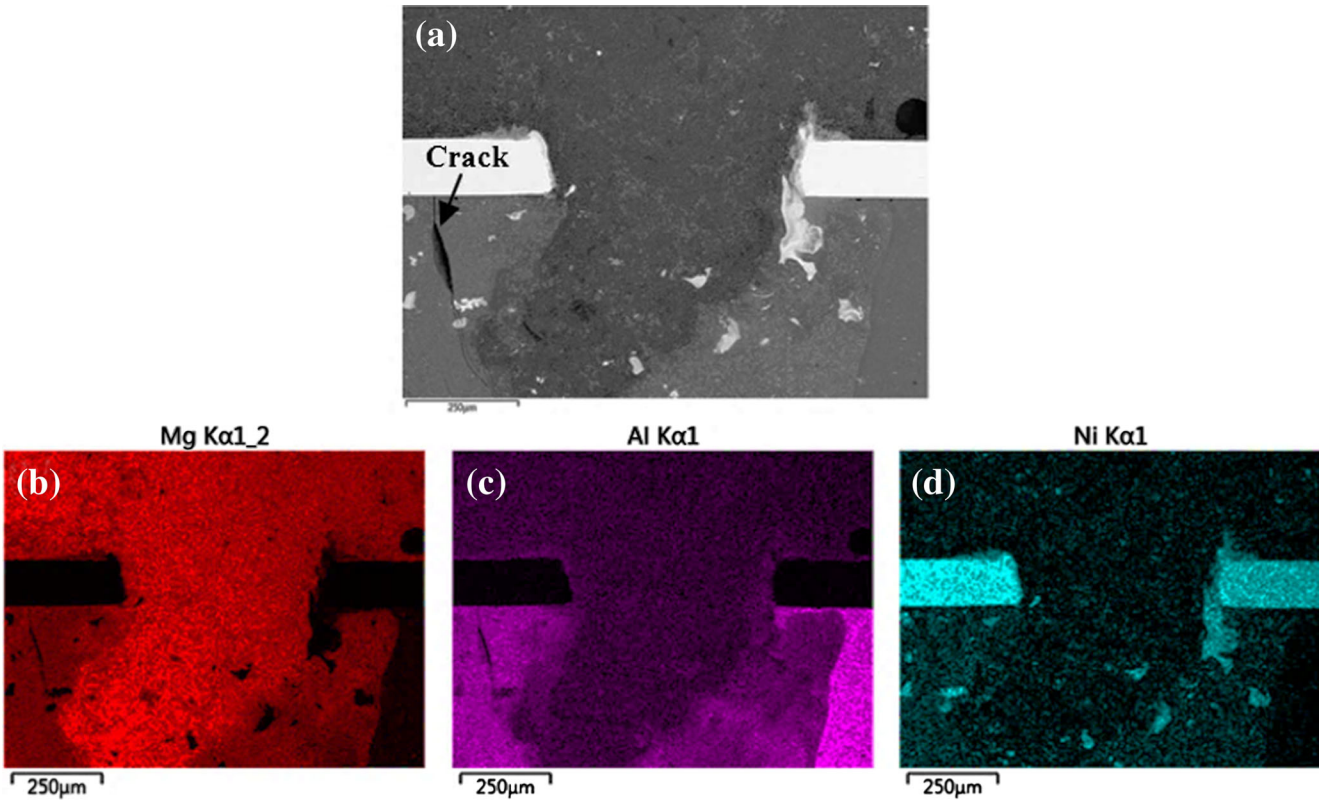

Fig. 7 **a** Overview of the interfacial area and the image of the distribution maps of major elements. **b** Map of element Mg. **c** Map of element Al. **d** Map of element Ni

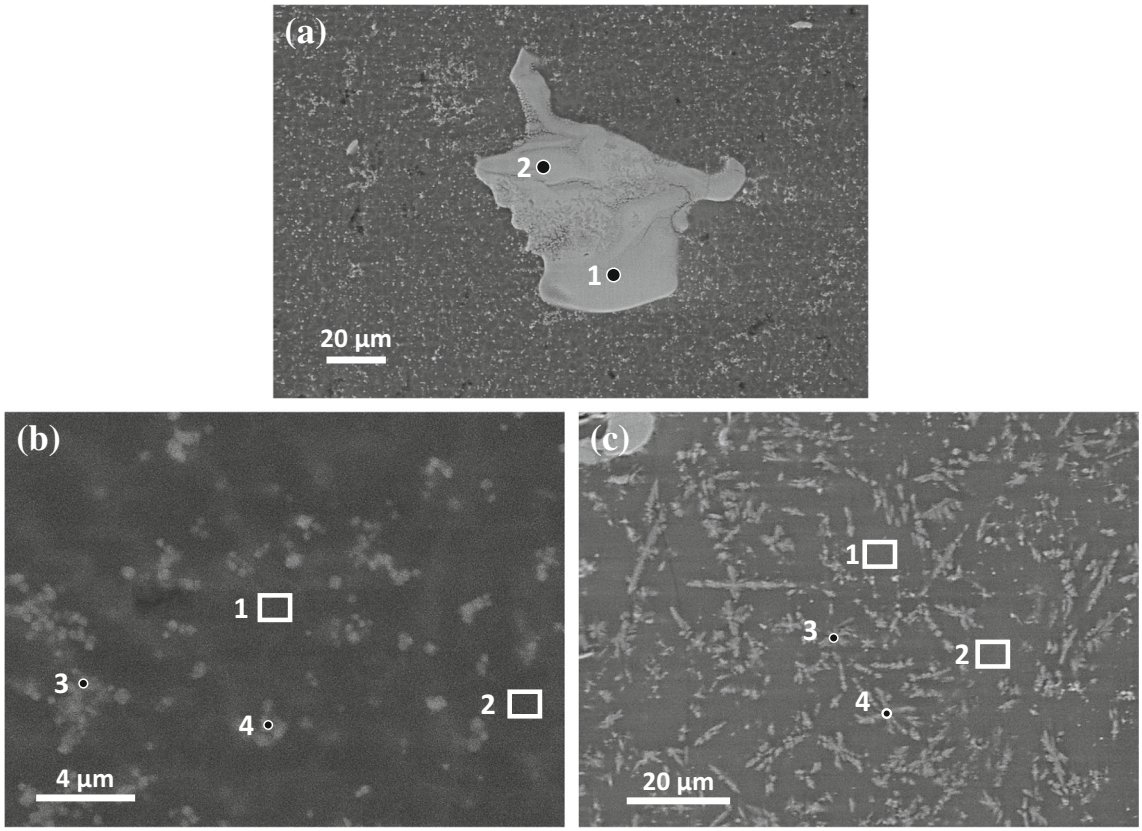

Fig. 8 SEM images of the **a** Ni island, **b** primary interface and **c** secondary interface

The elemental mapping also shows no interaction occurred between the Mg and Al base metals with the Ni foil where melting is absent. However, where the melted Ni foil islands are present, these areas have preferential interaction between Al and not with Mg. This compliments well with the thermodynamic calculation above in Figs. 2 and Fig. 3, where the Al-Ni formation enthalpy consistently has a much higher negative value compared to Al-Mg and Mg-Ni formation enthalpy values.

Figure 8 and Table 5 show the SEM image and EDS analysis of the Ni island, primary interface and secondary interface, respectively. EDS elemental analysis of the Ni island shows possible NiAl compounds. The dark region of primary interface indicates α-Mg due to the high percentage of Mg in area 1 and 2, while the bright region could not be identified since the region is too small to get an accurate elemental analysis and the high percentage of Mg may be due to the detector picking up signals from the periphery of the bright particles. However, other sources indicate that these are NiAl particles [44]. Further investigation is needed to precisely identify these particles.

The EDS data of the secondary interface on the other hand show an Al-dominant phase. For area 1 and 2, the main secondary interface compound is an Al-Mg-based IMC. The bright particles of area 3 and 4 show a significant increase in Ni. Through the Al-Mg-Ni phase diagram [68], the possible phase is Ni_2Al_3 with dissolved Mg. It is therefore evident from Table 5 that the crack observed in Fig. 7 propagated in the Al-Mg reaction region, which confirms the brittle nature of the Al-Mg IMCs [19, 21].

Table 5 Elemental composition of Ni island, primary interface, and secondary interface (at%)

Region	Area	Al	Ni	Mg
Ni island	1	41.68	55.26	2.84
	2	46.20	49.72	4.07
Primary interface	1	15.41	0.37	83.57
	2	12.57	0.95	85.91
	3	23.94	1.98	73.01
	4	20.12	1.56	77.36
Secondary interface	1	66.06	1.27	30.63
	2	56.17	0.73	40.60
	3	71.79	10.87	15.73
	4	73.44	9.90	14.77

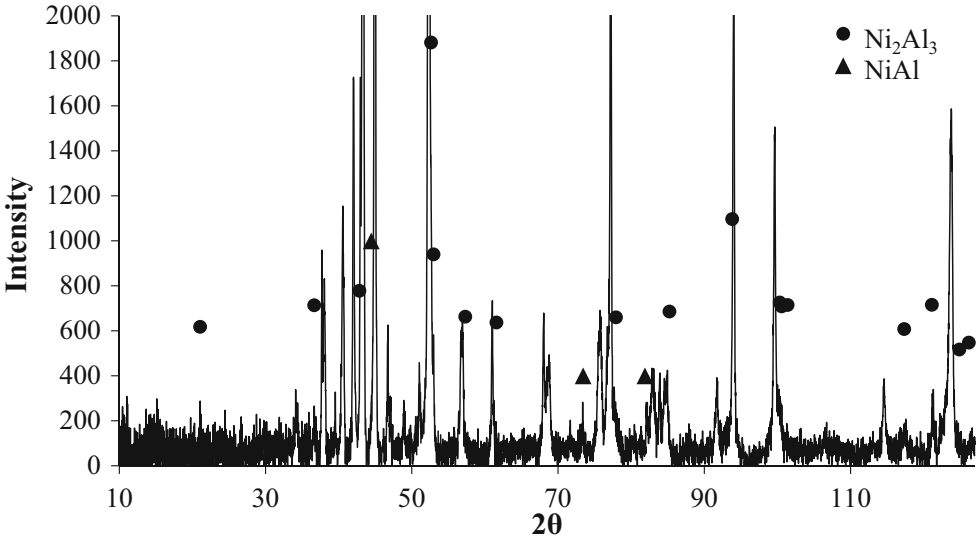

Fig. 9 XRD spectrum of detected compounds at the weld region

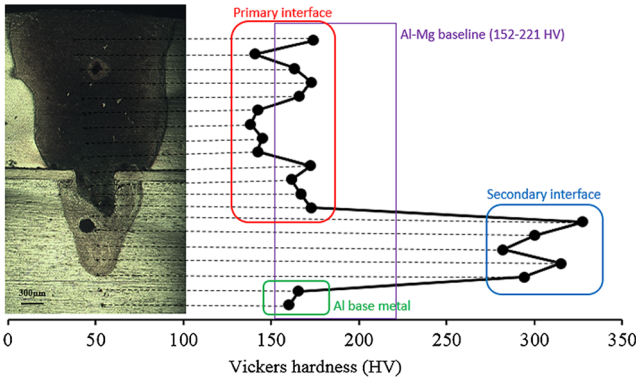

Fig. 10 Hardness profile throughout fusion zone interface

Figure 9 shows the XRD spectrum of detected compounds in the weld region. Other than the pure Al/Mg peaks and Al-Mg IMCs generally present in Al-Mg welding interface (not highlighted), Ni_2Al_3 and NiAl compounds were also detected. However, most of these peaks are either weak or overlapping with other more distinct peaks. This is due to the limited area of the Ni_2Al_3/NiAl particles compared to the whole weld region.

To validate the hardness of the primary and secondary interface, a vertical hardness profile was conducted as shown in Fig. 10. The primary interface shows a similar low hardness value compared to the Al base metal and the baseline values discussed in Table 3, while the secondary interface consistently shows a much higher hardness value compared to the baseline. The Ni interlayer has successfully minimized Al-Mg IMC formation by forming an α-Mg + NiAl compound in the primary interface to enhance the joint ductility. However, the brittle interface could not be completely prevented since the secondary interface consists of brittle Ni_2Al_3- and Al-Mg-based compounds. Through parameter optimization, the secondary interface could be further minimized in future researches.

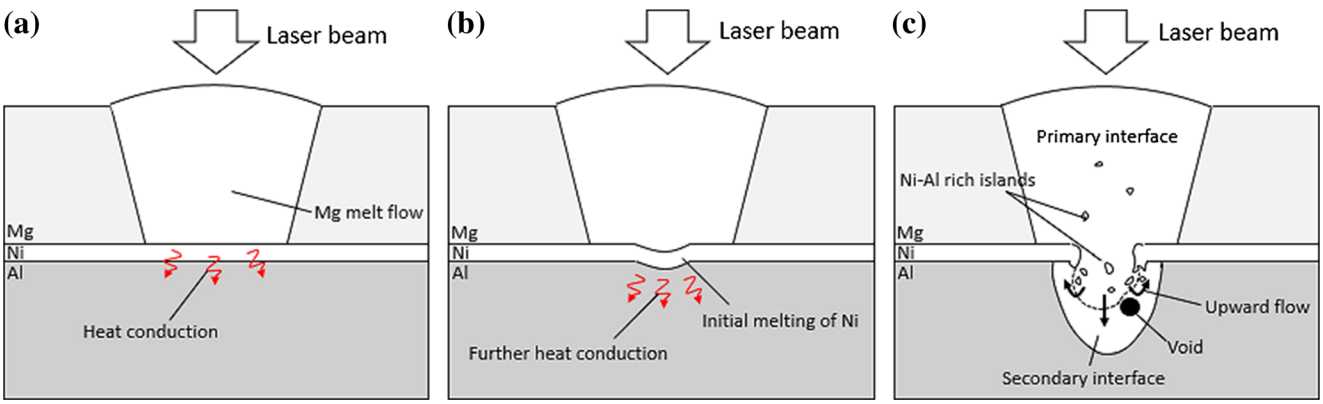

Fig. 11 Interface formation mechanism. **a** Initial Mg melting stage. **b** Ni foil melting stage. **c** Final Al melting and IMC formation stage

3.3 Interface formation mechanism

The interface formation mechanism of the laser welding process can be deduced in three stages, namely the magnesium melting stage, the Ni foil melting stage, and finally the aluminum melting stage. A schematic of the stages can be seen in Fig. 11. In the first stage, laser beam irradiates the upper magnesium sheet to form a molten pool. Due to high melting point, Ni retains its solid form but conducts heat to the lower Al sheet. In the meantime, the Mg liquid wets the Ni interlayer and promoted diffusion of Ni atoms in the Mg liquid. Next, the Ni interlayer begins to melt and dispersed throughout the fusion zone in the form of Ni-Al rich islands while the Mg melt also penetrates to the bottom sheet. Upon cooling, Ni preferentially begins to interact with Al in the Mg alloy matrix because of the higher negative ΔG value to form the ductile α-Mg + NiAl primary interface. Finally, the melted lower aluminum sheet mix with the molten magnesium from the top sheet to form Al-Mg rich + Ni_2Al_3 brittle secondary interface. This is because the diffusion rate of Mg to the Al matrix is higher than that of Ni to Al [69]. Ni-rich islands are dispersed throughout the primary and secondary interface due to the molten metal flow in the fusion zone.

4 Conclusion

By critically reviewing the recent research progress, the present manuscript has proposed that future work should be focused on improving the addition of metallic interlayer method due to its simplicity compared to other available techniques. To systematically select a suitable interlayer, a general 3-step guideline is proposed through the understanding of the basic concepts of thermodynamics and mechanical property as follows:

> Step 1: Thermodynamic assessments through formation enthalpy (ΔH) and Gibbs energy of compound (ΔG).
> Step 2: Mechanical property assessment through compound's ductility. In this step, other processing aspect such as accessibility and cost are also considered.
> Step 3: Feasibility study through empirical trials to optimize welding parameters.

A sample case study using Ni foil interlayer has evidently proven that the brittle Al-Mg interface could be substituted with a more ductile interface. Therefore, the 3-step guideline provided above has shown to be reliable. Utilization of this guideline could essentially open enormous potential to be undertaken in the field of Al-Mg welding research and can enable researchers to focus on specific metals to further improve Al-Mg joints. By careful selection and optimized welding parameters, an interface with a joint that ensures consistent strength and toughness could be achieved in the near future.

Acknowledgements The authors are grateful to the Ministry of Education Malaysia, Universiti Malaysia Pahang and Centre for Advanced Mechanical Joining, University of Waterloo for providing research funding. Support from the National Sciences and Engineering Research Council of Canada is also greatly appreciated.

References

1. Bergmann JP, Schuerer R, Ritter K (2013) Friction stir welding of tailored blanks of aluminum and magnesium alloys. Key Eng Mater 549:492–499. https://doi.org/10.4028/www.scientific.net/KEM.549.492
2. Shigematsu I, Kwon Y-J, Saito N (2009) Dissimilar friction stir welding for tailor-welded blanks of aluminum and magnesium alloys. Mater Trans 50:197–203. https://doi.org/10.2320/matertrans.MER2008326
3. Bhagwan AV, Kridli GT (2004) Formability improvement in aluminum tailor-welded blanks via material combinations. J Manuf Process 6:134–140
4. Tusek J, Kampus Z, Suban M (2001) Welding of tailored blanks of different materials. J Mater Process Technol 119:180–184
5. Kumar N, Yuan W, Mishra RS (2015) Friction stir welding of dissimilar alloys and materials. Butterworth-Heinemann, Oxford
6. Liu L, Ren D, Liu F (2014) A review of dissimilar welding techniques for magnesium alloys to aluminum alloys. Mater (Basel) 7:3735–3757. https://doi.org/10.3390/ma7053735
7. Baker H, Okamoto H (1995) Alloy phase diagrams, 9th edn. ASM International, Novelty
8. Kou S (2003) Welding metallurgy. Wiley, Hoboken
9. Borrisutthekul R, Miyashita Y, Mutoh Y (2005) Dissimilar material laser welding between magnesium alloy AZ31B and aluminum alloy A5052-O. Sci Technol Adv Mater 6:199–204. https://doi.org/10.1016/j.stam.2004.11.014
10. Liu L, Liu X, Liu S (2006) Microstructure of laser-TIG hybrid welds of dissimilar Mg alloy and Al alloy with Ce as interlayer. Scr Mater 55:383–386. https://doi.org/10.1016/j.scriptamat.2006.04.025
11. Liu L, Wang H, Song G, Ye J (2007) Microstructure characteristics and mechanical properties of laser weld bonding of magnesium alloy to aluminum alloy. J Mater Sci 42:565–572. https://doi.org/10.1007/s10853-006-1068-6
12. Liu LM, Wang HY, Zhang ZD (2007) The analysis of laser weld bonding of Al alloy to Mg alloy. Scr Mater 56:473–476. https://doi.org/10.1016/j.scriptamat.2006.11.034
13. Wang H, Liu L, Zhu M, Wang H (2007) Laser weld bonding of A6061Al alloy to AZ31B Mg alloy. Sci Technol Weld Join 12:261–265. https://doi.org/10.1179/174329307X159784
14. Miyashita Y, Borrisutthekul R, Chen J, Mutoh Y (2007) Application of twin laser beam on AZ31-A5052 dissimilar metals welding. Key Eng Mater 353–358:1956–1959
15. Liu LM, Wang HY (2009) The effect of the adhesive on the microcracks in the laser welded bonding Mg to Al joint. Mater Sci Eng A 507:22–28. https://doi.org/10.1016/j.msea.2008.11.061
16. Chang WS, Rajesh SR, Chun CK, Kim HJ (2011) Microstructure and mechanical properties of hybrid laser-friction stir welding between AA6061-T6 Al alloy and AZ31 Mg alloy. J Mater Sci Technol 27:199–204. https://doi.org/10.1016/S1005-0302(11)60049-2

17. Wang HY, Liu LM, Jia ZY (2011) The influence of adhesive on the Al alloy in laser weld bonding Mg-Al process. J Mater Sci 46: 5534–5540. https://doi.org/10.1007/s10853-011-5498-4
18. Liu L, Wang H (2011) Microstructure and properties analysis of laser welding and laser weld bonding Mg to Al joints. Metall Mater Trans A Phys Metall Mater Sci 42:1044–1050. https://doi.org/10.1007/s11661-010-0521-y
19. Qi X, Liu L (2012) Fusion welding of Fe-added lap joints between AZ31B magnesium alloy and 6061 aluminum alloy by hybrid laser-tungsten inert gas welding technique. Mater Des 33:436–443. https://doi.org/10.1016/j.matdes.2011.04.046
20. Scherm F, Bezold J, Glatzel U (2012) Laser welding of Mg alloy MgAl3Zn1 (AZ31) to Al alloy AlMg3 (AA5754) using ZnAl filler material. Sci Technol Weld Join 17:364–367. https://doi.org/10.1179/136217112X13333824902080
21. Gao M, Mei S, Li X, Zeng X (2012) Characterization and formation mechanism of laser-welded Mg and Al alloys using Ti interlayer. Scr Mater 67:193–196. https://doi.org/10.1016/j.scriptamat.2012.04.015
22. Wang H, Liu L, Liu F (2013) The characterization investigation of laser-arc-adhesive hybrid welding of Mg to Al joint using Ni interlayer. Mater Des 50:463–466. https://doi.org/10.1016/j.matdes.2013.02.085
23. Wang HY, Zhang ZD, Liu LM (2013) The effect of galvanized iron interlayer on the intermetallics in the laser weld bonding of Mg to Al fusion zone. J Mater Eng Perform 22:351–357. https://doi.org/10.1007/s11665-012-0260-x
24. Hajjari E, Divandari M, Razavi SH et al (2011) Dissimilar joining of Al Mg light metals by compound casting process. J Mater Sci 46: 6491–6499
25. Yamamoto N, Liao J, Watanabe S, Nakata K (2009) Effect of intermetallic compound layer on tensile strength of dissimilar friction-stir weld of a high strength Mg alloy and Al alloy. Mater Trans 50: 2833–2838. https://doi.org/10.2320/matertrans.M2009289
26. Zhang H, Dai X, Feng J (2014) Interfacial microstructure and mechanical properties of Al/Mg butt joints made by MIG welding process with Zn-Cd alloy as interlayer. J Wuhan Univ Technol Mater Sci Ed 29:1258–1264. https://doi.org/10.1007/s11595-014-1078-1
27. Morishige T, Kawaguchi A, Tsujikawa M et al (2008) Dissimilar welding of Al and Mg alloys by FSW. Mater Trans 49:1129–1131. https://doi.org/10.2320/matertrans.MC200768
28. Sato YS, Park SHC, Michiuchi M, Kokawa H (2004) Constitutional liquation during dissimilar friction stir welding of Al and Mg alloys. Scr Mater 50:1233–1236. https://doi.org/10.1016/j.scriptamat.2004.02.002
29. Penner P (2013) Resistance spot welding of Al to Mg with different interlayers. University of Waterloo
30. Sun M, Behravesh SB, Wu L et al (2016) Fatigue behavior of dissimilar Al 5052 and Mg AZ31 resistance spot welds with Sn-coated steel interlayer. Fatigue Fract Eng Mater Struct:1–11. https://doi.org/10.1111/ffe.12563
31. Chang W-S, Rajesh SR, Chun C-K, Kim H-J (2011) Microstructure and mechanical properties of hybrid laser-friction stir welding between AA6061-T6 Al alloy and AZ31 Mg alloy. J Mater Sci Technol 27:199–204. https://doi.org/10.1016/S1005-0302(11)60049-2
32. Dai X, Zhang H, Zhang H et al (2016) Arc assisted ultrasonic seam welding of Mg/Al joints with Zn interlayer. Mater Sci Technol 32: 1–9. https://doi.org/10.1179/1743284715Y.0000000070
33. Hao X, Song G (2008) Spectral analysis of the plasma in low-power laser/arc hybrid welding of magnesium alloy. IEEE Trans Plasma Sci 37:76–82. https://doi.org/10.1109/TPS.2008.2005720
34. Patel VK, Bhole SD, Chen DL (2012) Improving weld strength of magnesium to aluminium dissimilar joints via tin interlayer during ultrasonic spot welding. Sci Technol Weld Join 17:342–347. https://doi.org/10.1179/1362171812Y.0000000013
35. Panteli A, Chen YC, Strong D et al (2012) Optimization of aluminium-to-magnesium ultrasonic spot welding. JOM 64:414–420. https://doi.org/10.1007/s11837-012-0268-6
36. Shang J, Wang K, Zhou Q et al (2012) Microstructure characteristics and mechanical properties of cold metal transfer welding Mg/Al dissimilar metals. Mater Des 34:559–565. https://doi.org/10.1016/j.matdes.2011.05.008
37. Penner P, Liu L, Gerlich A, Zhou Y (2013) Feasibility study of resistance spot welding of dissimilar Al/Mg combinations with Ni based interlayers. Sci Technol Weld Join 18:541–550. https://doi.org/10.1179/1362171813Y.0000000129
38. Liu F, Ren D, Liu L (2013) Effect of Al foils interlayer on microstructures and mechanical properties of Mg–Al butt joints welded by gas tungsten arc welding filling with Zn filler metal. Mater Des 46:419–425. https://doi.org/10.1016/j.matdes.2012.10.012
39. Panteli A, Robson JD, Chen YC, Prangnell PB (2013) The effectiveness of surface coatings on preventing interfacial reaction during ultrasonic welding of aluminum to magnesium. Metall Mater Trans A Phys Metall Mater Sci 44:5773–5781. https://doi.org/10.1007/s11661-013-1928-z
40. Zhang HT, Dai XY, Feng JC (2014) Joining of aluminum and magnesium via pre-roll-assisted A-TIG welding with Zn interlayer. Mater Lett 122:49–51. https://doi.org/10.1016/j.matlet.2014.02.008
41. Liu F, Wang H, Liu L (2014) Characterization of Mg/Al butt joints welded by gas tungsten arc filling with Zn–29.5Al–0.5Ti filler metal. Mater Charact 90:1–6. https://doi.org/10.1016/j.matchar.2014.01.010
42. Penner P, Liu L, Gerlich A, Zhou Y (2014) Dissimilar resistance spot welding of aluminum to magnesium with Zn-coated steel interlayers. Weld J 93:225s–231s
43. Zhang Y, Luo Z, Li Y et al (2015) Microstructure characterization and tensile properties of Mg/Al dissimilar joints manufactured by thermo-compensated resistance spot welding with Zn interlayer. Mater Des 75:166–173. https://doi.org/10.1016/j.matdes.2015.03.030
44. Sun M, Niknejad ST, Zhang G et al (2015) Microstructure and mechanical properties of resistance spot welded AZ31/AA5754 using a nickel interlayer. Mater Des 87:905–913. https://doi.org/10.1016/j.matdes.2015.08.097
45. Sun M, Niknejad ST, Gao H et al (2016) Mechanical properties of dissimilar resistance spot welds of aluminum to magnesium with Sn-coated steel interlayer. Mater Des 91:331–339. https://doi.org/10.1016/j.matdes.2015.11.121
46. Miedema AR, Chatel PF de (1979) A semiempirical approach to the heat of formation problem. Theory Alloy Phase Form: 344-389
47. Miedema AR, de Chatel PF, de Boer FR (1980) Cohesion in alloys—fundamentals of a semi-empirical model. Phys B+ C 100:1–28. https://doi.org/10.1016/0378-4363(80)90054-6
48. Miedema AR, Niessen AK, de Boer FR et al (1989) Cohesion in metals: transition metal alloys. North-Holland, Amsterdam
49. Bakker H, Miedema AR (1998) Enthalpies in alloys: Miedema's semi-empirical model. Trans Tech Publications, Zurich
50. Zhang RF, Liu BX (2002) Proposed model for calculating the standard formation enthalpy of binary transition-metal systems. Appl Phys Lett 81:1219–1221
51. Zhang RF, Sheng SH, Liu BX (2007) Predicting the formation enthalpies of binary intermetallic compounds. Chem Phys Lett 442:511–514
52. Zhang RF, Rajan K (2014) Statistically based assessment of formation enthalpy for intermetallic compounds. Chem Phys Lett 612: 177–181
53. Gilman JJ (2009) Chemistry and physics of mechanical hardness. Wiley, Hoboken

54. Kattner UR, Boettinger WJ (1992) Thermodynamic calculation of the ternary TiAlNb system. Mater Sci Eng A 152:9–17. https://doi.org/10.1016/0921-5093(92)90039-4
55. Jia BR, Liu LB, Yi DQ et al (2008) Thermodynamic assessment of the Al-Mg-Sm system. J Alloys Compd 459:267–273
56. Ansara I, Dupin N, Lukas HL, Sundman B (1997) Thermodynamic assessment of the Al-Ni system. J Alloys Compd 247:20–30. https://doi.org/10.1016/S0925-8388(96)02652-7
57. Roine A (2002) HSC Chemistry 5(11):76
58. Weaver MI, Stevenson ME, Bradt RC (2003) Knoop hardness anisotropy and the indentation size effect on the (100) of single crystal NiAl. Mater Sci Eng A 345:113–117. https://doi.org/10.1016/S0921-5093(02)00454-9
59. Ke L, Huang C, Xing L, Huang K (2010) Al-Ni intermetallic composites produced in situ by friction stir processing. J Alloys Compd 503:494–499
60. Konieczny M, Mola R, Thomas P, Kopcial M (2011) Processing, microstructure and properties of laminated Ni-intermetallic composites synthesised using Ni sheets and Al foils. Arch Metall Mater 56:693–702
61. Kumar KG, Sivarao ATJS (2011) A novel intermetallic nickel aluminide (Ni3Al) as an alternative automotive body material. Int J Eng Technol 11:208–215
62. Song YK, R a V (2001) Phase equilibria and intermetallic phases in the Ni-Si-Mg ternary system. Metall Mater Trans A 32:5–18. https://doi.org/10.1007/s11661-001-0246-z
63. Nasiri AM, Weckman DC, Zhou Y (2013) Interfacial microstructure of diode laser brazed AZ31B magnesium to steel sheet using a nickel interlayer. Weld J 92:1–10
64. Qi X, Song G (2010) Interfacial structure of the joints between magnesium alloy and mild steel with nickel as interlayer by hybrid laser-TIG welding. Mater Des 31:605–609. https://doi.org/10.1016/j.matdes.2009.06.043
65. Matsunawa A, Mizutani M, Katayama S, Seto N (2003) Porosity formation mechanism and its prevention in laser lap welding. Weld Int 17:431–437. https://doi.org/10.1016/j.jmatprotec.2014.03.011
66. Haboudou A, Peyre P, Vannes AB, Peix G (2003) Reduction of porosity content generated during Nd: YAG laser welding of A356 and AA5083 aluminium alloys. Mater Sci Eng A 363:40–52. https://doi.org/10.1016/S0921-5093(03)00637-3
67. Zhao H, White DR, DebRoy T (1999) Current issues and problems in laser welding of automotive aluminum alloys. Int Mater Rev 44:238–266
68. Raghavan V (2009) Al-Mg-Ni (Aluminum-Magnesium-Nickel). J Phase Equilibria Diffus 30:274–275. https://doi.org/10.1007/s11669-009-9519-9
69. Du Y, Chang YA, Huang B et al (2003) Diffusion coefficients of some solutes in fcc and liquid Al: critical evaluation and correlation. Mater Sci Eng A 363:140–151. https://doi.org/10.1016/S0921-5093(03)00624-5